Instituto Nacional de Investigación y Tecnología Agraria y Alimentaria (INIA)
Available online at www.inia.es/sjar

Spanish Journal of Agricultural Research 2007 5(4), 460-469
ISSN: 1695-971-X

Numerical modeling of cavitating flows for simple geometries using FLUENT V6.1

G. Palau-Salvador[1]*, P. González-Altozano[2] and J. Arviza-Valverde[2]

[1] *Departamento de Ingeniería Rural y Agroalimentaria. ETS Ingenieros Agrónomos. Universidad Politécnica de Valencia. Cno. de Vera, s/n. 46022 Valencia. Spain*

[2] *Departamento de Ingeniería Rural y Agroalimentaria. ETS del Medio Rural y Enología. Universidad Politécnica de Valencia. Cno. de Vera, s/n. 46022 Valencia. Spain*

Abstract

Cavitation is a phenomenon that can be present in several agro-forestry applications such as irrigation pressure-reducing valves, sprinkler orifices or even in the flow through xylem vessels inside plants. In the present research, numerical predictions of cavitation in a series of orifices, nozzles and venturis were compared to experimental measurements to show the possibilities and performances of the new cavitation model in the commercial Computational Fluid Dynamics (CFD) code FLUENT V6.1. A flashing study is also presented for the nozzle case. Model predictions for the orifice cases accurately capture cavitation inception and its influence on the orifice discharge coefficient. However, when an unsteady flow is modeled, the cavitation phenomenon is not simulated properly and leads to a steady situation. In general, the new cavitation model in FLUENT V6.1 provides very reliable simulation for easy geometries when steady flow is assumed.

Additional key words: computational fluid dynamic technique, flow simulation, steady flow, unsteady flow.

Resumen

Modelo numérico de cavitación para geometrías sencillas utilizando FLUENT V6.1

Los procesos de cavitación tienen relevancia en diferentes aspectos del área agroforestal, como en válvulas reductoras de presión para riego, chorros en aspersores e incluso en el flujo de savia en el xilema de las plantas. En este trabajo se ha validado el nuevo modelo de cavitación incluido en el programa comercial de mecánica de fluidos computacional FLUENT V6.1 en varios orificios, estrechamientos y venturis, comparando los resultados experimentales con los obtenidos por el modelo. También se presenta un estudio del fenómeno «flashing» producido en el estrechamiento. Las predicciones del modelo en el caso de los orificios muestran una buena estimación del momento de inicio de la cavitación así como de su desarrollo, estimado con el coeficiente de descarga del orificio. Sin embargo, cuando se trata de modelar el flujo en estado no estacionario, el proceso de cavitación no es simulado correctamente conduciendo a una situación estacionaria. De todo ello podemos concluir que el nuevo modelo de cavitación simula adecuadamente la cavitación en el flujo a través de geometrías sencillas, como los orificios y estrechamientos, en estado estacionario.

Palabras clave adicionales: flujo estacionario, flujo no estacionario, mecánica de fluidos computacional, simulación de flujo.

Introduction

According to Knapp *et al.* (1970), cavitation can be classified into several different regimes: traveling, fixed and vortex cavitation. In each, the onset of cavitation occurs due to flow acceleration and consequently an accompanying drop in pressure at a point within the liquid flow that causes vapor bubble formation. Bubbles travel downstream until the increase of pressure causes the bubbles to implode. This two-step process is known as cavitation. Cavitating flows often lead to performance degradation and structural damage to many hydraulic devices. These effects are related to the size, the time-averaged shapes of the vaporized structures and their area of influence.

Pumps, valves, propellers, nozzles and numerous other devices can be affected by cavitation. For several

* Corresponding author: guipasal@agf.upv.es
Received: 19-01-06; Accepted: 18-10-07.

G. Palau-Salvador and J. Arviza-Valverde ares members of the SEA.

years, numerous researchers have been obtaining experimental data about cavitation inception and development for flow elements such as nozzles, orifices, venturis and Schiebe headforms (Nurick, 1976; Abuaf *et al.*, 1981; Meyer *et al.*, 1992; Stutz and Reboud, 1997).

The use of CFD (Computational Fluid Dynamics) in designing engineering devices has increased over the past few years due to the availability of commercial codes featuring state-of-the-art robust models and the ability to run the code on desktop PC's. Agro-forestry engineering applications of CFD have also increased in recent years. Palau-Salvador *et al.* (2004) and Wei *et al.* (2006) are excellent examples of this, as both used the commercial code FLUENT V6.1 (FLUENT, 2001) to predict the hydrodynamic behavior inside the labyrinth of an in-line emitter. Other applications in agricultural applications range from food industry processes (Norton and Sun, 2006; Smale *et al.*, 2006) to farm and greenhouse ventilation (Norton *et al.*, 2007).

Evaluating cavitation requires a multiphase flow model. This model may be based on either a separate treatment of the continuum and particulate phase using an Eulerian/Lagrangian approach (Farrel, 2003; Cerutti *et al.*, 2000) or as a homogeneous fluid using an Eulerian/Eulerian approach (Kubota *et al.*, 1992; Singhal *et al.,* 2002; Xing and Frankel, 2002). Many studies have contributed to improving CFD cavitation models to obtain a more realistic approach to simulating vapor formation, which allows cavitation characteristics to be predicted in the areas most affected inside the hydraulic devices.

A flashing flow is a non-recoverable cavitating flow. This phenomenon is very important in flows with strong thermodynamic effects, such as light water nuclear reactors during accidental loss of cooling (Xu *et al.*, 1997). There have been several experimental studies of flashing flows (Abuaf *et al.*, 1981) and prediction modeling studies (Elias and Chambre, 2000; Muñoz-Cobo *et al.*, 2000). Nevertheless, all the studied models presented considerable differences between their predictions and experimental results, such as the study carried out with the commercial code FLUENT V5.0 by Xing (2002), which concluded that the cavitation model in this code underestimated the upstream pressure in a flashing flow.

Cavitation in agricultural applications plays an important role in the efficient performance of valves (Palau-Salvador *et al.*, 2005), venturis (Manzano and Palau-Salvador, 2005), flowmeters (Palau *et al.*, 2004), sprinklers (Pascal *et al.*, 2006) located in pressure irrigation systems and even in xylem vessels of plants when sap travels long distances from root to leaves (Cochard *et al.*, 2007 or Maheraly *et al.*, 2006).

The objective of this work is to study the characteristics and performance of the new cavitation model of the commercial code FLUENT V6.1 for predicting cavitation in orifices, nozzles and venturis, in both steady and unsteady situations, highlighting their applications in rural environments. The ability of this new model to predict flashing flow is also investigated.

Cavitation model

General lines

The cavitation model of FLUENT V6.1 is based on the full cavitation model developed by Singhal *et al.* (2002). This model involves two phases and a certain fraction of non-condensable gases, whose mass fraction must be known in advance. This model takes into account the formation and collapse of the bubbles. This new code improves the old cavitation model in Fluent, where, for instance, bubbles were neither created nor destroyed. A comparison between the main characteristics of the cavitation model in FLUENT V5.0 and the new cavitation model of FLUENT V6.1 is presented in Table 1.

Numerical method

The model equations are solved using the solver in FLUENT V6.1. In all cases, a structured grid generated

The following symbols are used in this paper: C_c, C_e = Empirical constants for the vapor generation and collapse rates (dimensionless); C_d = Discharge coefficient (dimensionless); d = Exit diameter (m); D_i = Inlet diameter (m); f = Vapour fraction (dimensionless); g = Gravity acceleration (m s^{-2}); γ = Effective exchange coefficient (dimesionless); L = Length (m); L_i = Inlet length (m); $\dot{m}$ = Mass flow (kg s^{-1}); P = Pressure (Pa); P_0 = Upstream pressure (Pa); P_b = Exit pressure (Pa); P_{sat} = Liquid saturation vapor pressure (Pa); ρ = Fluid density (kg m^{-3}); ρ_l = Liquid density (kg m^{-3}); ρ_m = Mixture density (kg m^{-3}); ρ_v = Vapor density (kg m^{-3}); R_c, R_e = Vapor generation and collapse rates (kg m^{-3} s^{-1}); Σ = Cavitation number (dimensionless); σ = surface tension of the liquid (kg m^{-1}); t = Time (s); T = Temperature (K); τ = Stress tensor (Pa); v = Mean velocity (m s^{-1}); v_b = Mean velocity at the inlet (m s^{-1}); v_{ch} = Characteristic velocity (m s^{-1}); v_v = Velocity of the vapor phase (m s^{-1}); z = Height (m).

Table 1. Differences between old and new cavitation models in Fluent

Old cavitation model in FLUENT V5	New cavitation model in FLUENT V6.1
— The system under research involves only two phases.	— The system under research involves only two phases (liquid-vapour) and a certain fraction of separately modelled non-condensable gases.
— Bubbles are neither created nor destroyed.	— Both bubble formation (evaporation) and collapse (condensation) are considered in the model.
— The population or number of bubbles per volume unit must be known in advance.	— The mass fraction of non-condensable gases must be known in advance.

using GAMBIT 2.0 is used to mesh the domain. The momentum equations are discretized using both first and second order upwind scheme options. The turbulence models used were the standard k-ε, RNG k-ε or SST k-ω according to each particular case [See Launder and Spalding (1972) or Veersteg and Malalasekera (1995) for more information on this topic].

The governing equations were the mass conservation and the momentum balance equations. These were solved using the SIMPLE algorithm developed by Patankar (1980). On the one hand, the mass conservation equation is expressed for an incompressible and Newtonian fluid as:

$$\nabla \cdot v = 0 \qquad [1]$$

where v is the mean velocity and ∇ is the vector operator $\nabla = \frac{\partial}{\partial x} + \frac{\partial}{\partial y} + \frac{\partial}{\partial z}$. On the other hand, the momentum balance equation is formulated as:

$$\rho\left(\frac{\partial v}{\partial t} + (v\cdot\nabla)v\right) = -\rho g \nabla z - \nabla P + \nabla \tau^{*} \qquad [2]$$

where ρ is the fluid density, $\partial v / \partial t$ is the local acceleration that is equal to zero for steady flow, g is the gravity acceleration, z is the height, P is the static pressure and ∇τ* stands for the divergence of the stress tensor. In this term, the number of unknowns turns out to be 13 (velocity components, pressure and stress field), which makes the above equation very difficult to solve. However, calculations are simplified by using the Navier-Stokes equations, which relate the stress field to fluid viscosity. In all the cases modelled a second order upwind scheme was used to discretize the equations involved. Normalized residuals set at six orders of magnitude were used for the convergence criteria. In each case, the boundary conditions and specific conditions of the runs were specified.

When the cavitation model is activated, the working fluid is assumed to be a mixture of three species (liquid, vapor and non-condensable gas). The vapour fraction, f, affects the fluid density and its governing equation is:

$$\frac{\partial}{\partial t}(\rho_m f) + \nabla \cdot (\rho_m v_v f) = \nabla \cdot (\gamma \nabla f) + R_e - R_c \qquad [3]$$

where ρ_m is the mixture density, f the mass fraction, ρv_v the velocity vector of the vapor phase and γ the effective exchange coefficient. The source terms R_e and R_c represent vapor generation and collapse rates, which can be expressed as a function of the main flow parameters. In fact, the expressions used in this cavitation model are functions of static pressure and are given by the two equations (Singhal *et al.*, 2002):

$$R_e = C_e \frac{v_{ch}}{\sigma} \rho_l \rho_v \sqrt{\frac{2(P_{sat} - P)}{3\rho_l}} (1 - f) \qquad [4]$$

$$R_c = C_c \frac{v_{ch}}{\sigma} \rho_l \rho_l \sqrt{\frac{2(P - P_{sat})}{3\rho_l}} f \qquad [5]$$

where C_e and C_c are empirical constants, v_{ch} a characteristic velocity, σ the surface tension of the liquid; ρ_l and ρ_v the liquid and vapor density; P the pressure and P_{sat} the liquid saturation vapor pressure at the working temperature. The Eq. [4] is used when ρ is smaller than P_{sat} and the Eq. [5] when ρ is greater than P_{sat}.

The new cavitation model provides a wider range of options than the old model. The turbulence model can be selected from all the Reynolds Average Navier Stokes possibilities. In the present study, different situations have been validated, choosing the option that leads to the best agreements with the experimental data extracted from the literature.

However, the model still has several limitations. First, its study is based on the Eulerian/Eulerian approach, so bubbles cannot be modelled as separate particles. Also, this model cannot be used together with the Large Eddy Simulation (LES) models. This limitation reflects the basic nature of the research efforts related to applying LES to simple cavitating flows such as jets (Cerutti *et al.*, 2000).

It is especially interesting that the FLUENT V6.1 cavitation model allows the use of a slip velocity between bubbles and liquid. However, this slip velocity was not considered in any of the models used in this study.

Cases studied

Several easy geometries were selected to test and validate the new cavitation model in FLUENT V6.1. These geometries included a circular orifice, a rectangular orifice, a nozzle and a rectangular venturi. In the nozzle, a study of the flashing phenomena was also addressed and an unsteady situation was studied in the rectangular venturi. Only CFD simulations were carried out. The experimental data, geometries and results were obtained from different papers in the bibliography: Nurick (1976) for the circular and rectangular orifices; Abuaf *et al.* (1981) for the nozzle; and Stutz and Reboud (2000) for the rectangular venturi. Schemes of all the modeled geometries are given in Figure 1. In Table 2 the possible agricultural application of the analyzed geometries are highlighted. More information about each particular case is provided in the following sections.

Case A: Circular orifice

The effect of cavitation in circular orifices was experimentally investigated by Nurick (1976). Cavitation occurs when the flow passes through a very small orifice, which produces a high differential pressure. This effect can be observed in hydraulic valves (Palau-Salvador *et al.*, 2005) or in flow-meters (Palau *et al.*, 2004). In Nurick's paper, a large number of experiments were carried out on different geometries, and the experimental results were compared to those obtained by modeling the same geometries. In the present paper, only the geometry shown in Figure 1 is presented, but good agreement was also obtained for the other geometries studied by Nurick (1976).

Table 2. Different examples of cavitation found in rural and irrigation applications

Circular (CASE A) and rectangular (CASE B) orifices
— Hydraulic control valves (Palau-Salvador *et al.,* 2005).
— Flow meters (Palau *et al.,* 2004).
Circular (CASE C) and rectangular (CASE D) venturi
— Fertirrigation devices (Manzano and Palau-Salvador, 2005).
— Water jets in sprinklers (Pascal *et al.,* 2006).

The turbulence models used were the standard k-ε and RNG k-ε. Both presented good results and no differences were detected between them in the prediction of cavitation in the circular orifice. The characteristic geometric parameters of the circular orifice studied were D/d = 2.88 and L/d = 20. Uniform inlet and outlet static pressure were adopted as boundary conditions. The exit pressure was fixed at 9,500 Pa and the upstream pressure varied, as in Nurick's experiments, between 3×10^8 and 2×10^5 Pa. The parameters used to validate the model were the cavitation number (Σ) and the discharge coefficient (C_d):

$$\text{Cavitation number: } \sum = \frac{P_o - P_{sat}}{P_o - P_b} \qquad [6]$$

Discharge coefficient:

$$C_d = \frac{\bar{v}_b}{\sqrt{2(P_o - P_b)/\rho}} = \frac{\dot{m}_{actual}}{\dot{m}_{ideal}} \qquad [7]$$

where P_o, P_{sat} and P_b are the upstream, vapor and exit pressure, respectively; v_b the velocity at the inlet; ρ the liquid density and $\dot{m}$ the mass flow.

An axysymmetric 2D domain with a structured grid of 42,860 nodes was finally used after testing mesh sensitivity by using finer meshes and verifying that there was no influence on the predicted mass flow.

The effect of a temperature increase in the model is shown in Figure 2. Although the temperature effect is small, the predicted C_d is consistently lower than the values found by Nurick (1976) when the cavitation number is greater than 1.6. In order to determine the reason for this difference, the same geometry was modeled with a different inlet pipe length (Fig. 3). C_d prediction was better when the length (L_i) was around 15 outlet diameters (15 d) with an error of < 5%, even when the cavitation number was > 1.6.

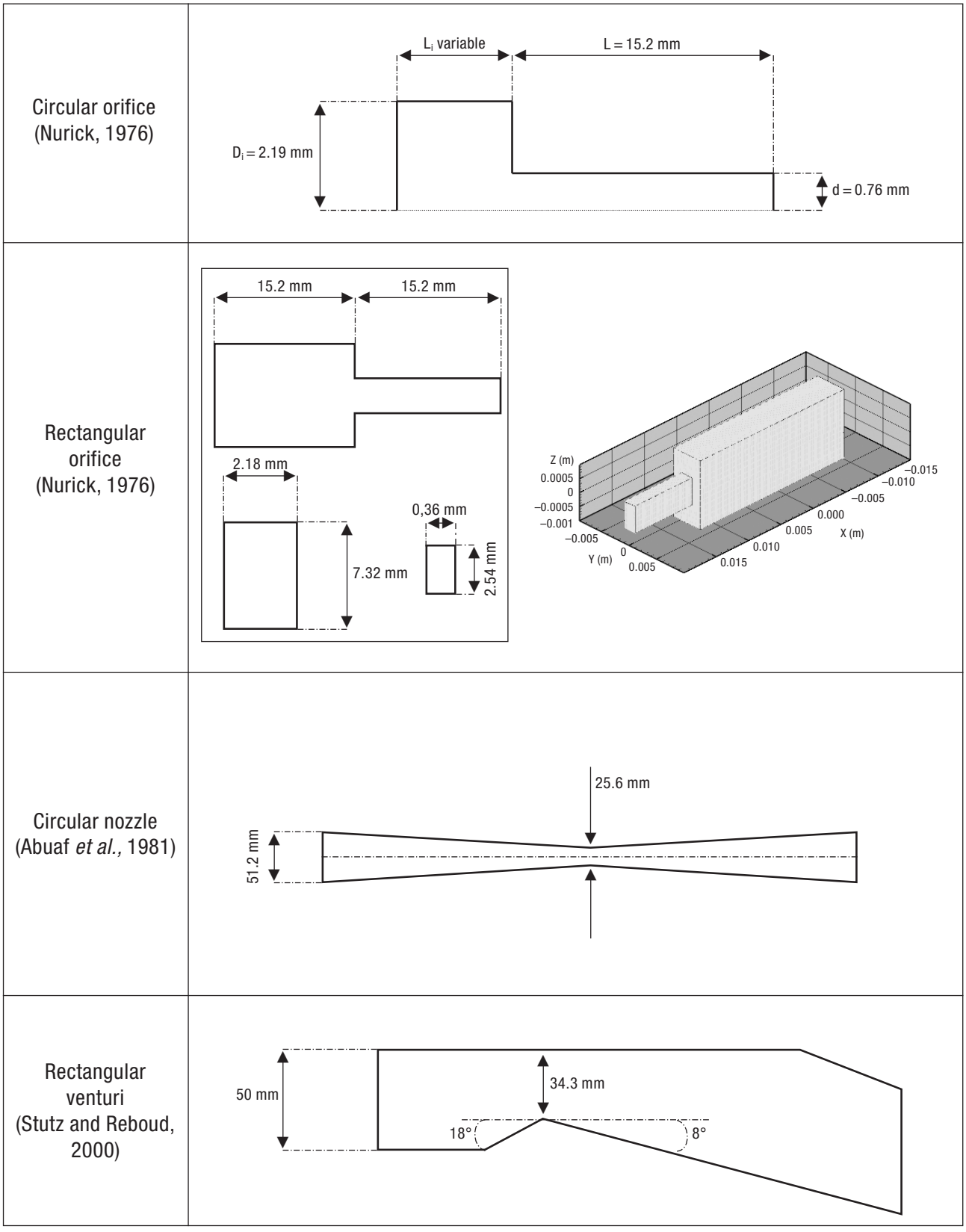

Figure 1. Summary of the geometries used for validating the new cavitation model of FLUENT V6.1.

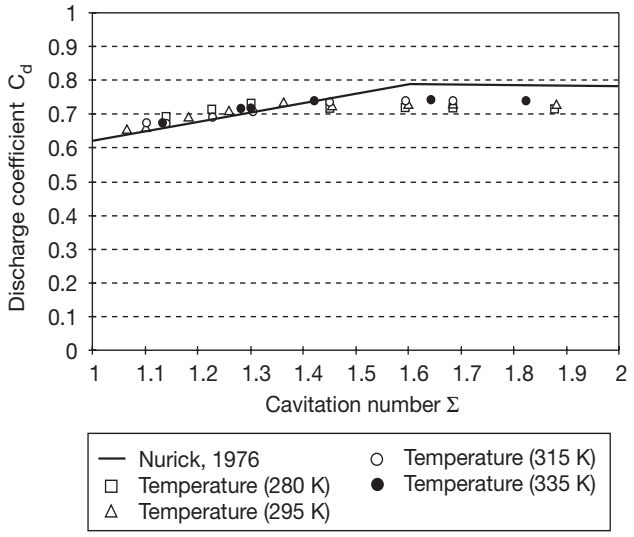

Figure 2. Effect of temperature on the C_d prediction of the circular orifice.

Case B: Rectangular orifice

As in the case of the circular orifice, Nurick's (1976) experimental data were used. The parameters used to validate the model were the same as in the case of the circular orifice: discharge coefficient (C_d) and cavitation number (Σ). The geometry of the rectangular orifice modeled is shown in Figure 1, and is relevant due to its relation with jet cavitation, as happens in control valves (Palau-Salvador *et al.*, 2005) or sprinkler guns (Pascal *et al.*, 2006).

The turbulence model used for this case was the SST k-ω model, since the predicted C_d for the rectangular orifice with the standard k-ε and RNG k-ε did not agree with the experimental results obtained by Nurick (1976), as shown in Figure 4. All solid boundaries were represented using no slip velocity conditions. With regard to the inlet and outlet boundaries, uniform static pressures were adopted. The downstream pressure was fixed at 9,500 Pa and the upstream pressure varied between 2×10^8 and 2×10^5 Pa, as in Nurick's assays. A 3D model was created with a symmetry boundary in the middle of the orifice. A structured mesh was considered. Several mesh sizes were used to check the grid sensitivity. The final mesh used featured 281,730 nodes, after checking that the prediction worsened with the coarsest grid and did not improve with the finest (Fig. 5). Mesh size effect on the vapor fraction prediction is shown in the symmetry plane in Figure 6. As can be seen, the coarse grid (33,948 cells) did not properly simulate the cavitation generated in the orifice outlet, so a finer mesh was needed in accordance with C_d prediction results (Fig. 5).

Cavitation predictions for the rectangular orifice were not as good as for the circular one. However, with a considerably refiner mesh (281,730 nodes), the model was in reasonable agreement with the experimental data obtained by Nurick (1976). The final error was < 10% when the cavitation number was < 1.3 and even lower with higher cavitation numbers.

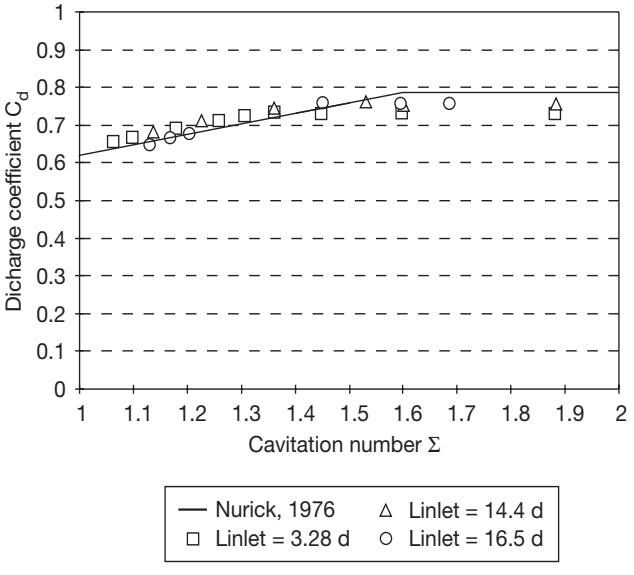

Figure 3. Effect of inlet pipe length on the C_d prediction of the circular orifice. Inlet lengths tested were 3.28, 14.4 and 16.5 times the outlet diameter (d).

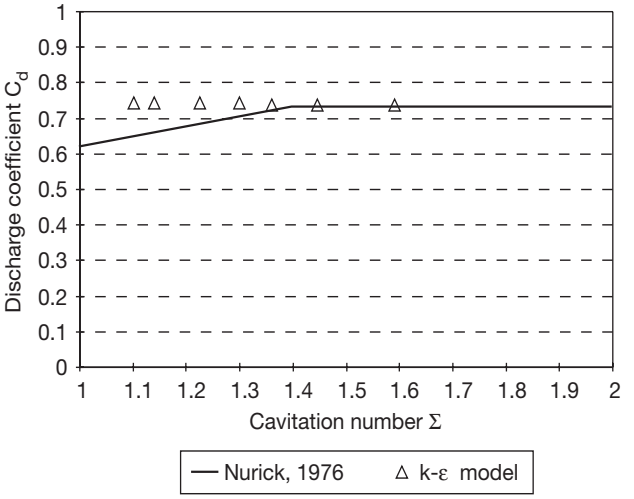

Figure 4. Prediction of C_d using the k-ε model compared with the experimental data obtained by Nurick (1976).

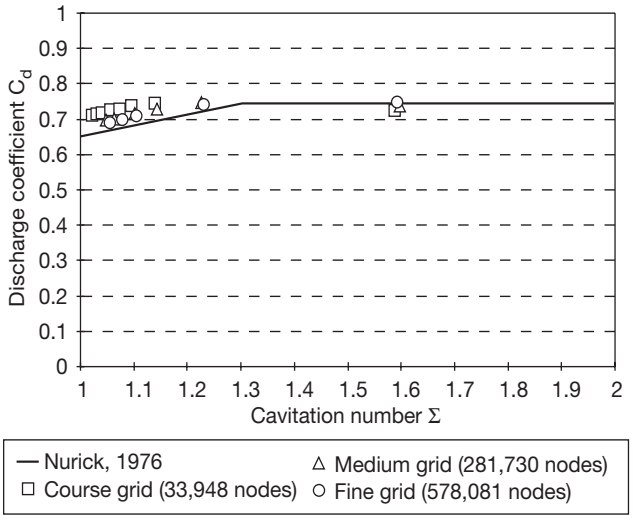

Figure 5. Effect of different mesh sizes on the C_d predictions in the rectangular orifice using SST k-ω model compared to the experimental data of Nurick (1976).

Case C: Nozzle (Flashing flow)

Flashing flow is very difficult to predict, as the void fraction does not recover downstream of the nozzle. A previous study on flashing flow modeling was carried out by Xing (2002) using the FLUENT V5. With this version, there was an underestimation of the upstream pressure and the downstream vapor fraction. With the new cavitation model used by FLUENT V6.1, better results were obtained when modeling this kind of flow.

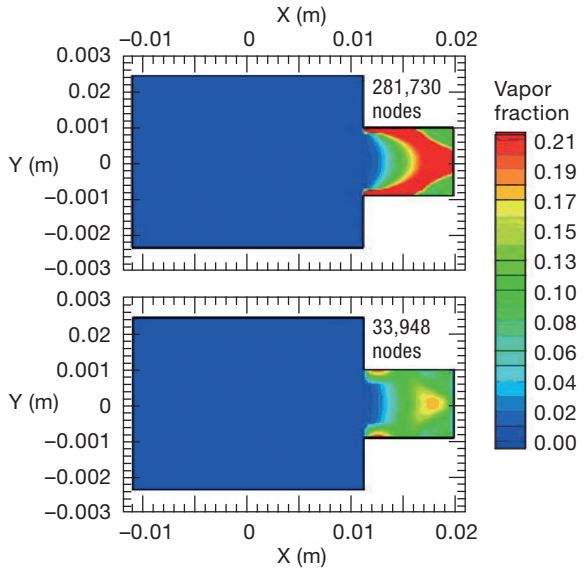

Figure 6. Vapor fraction in the rectangular orifice obtained with different mesh sizes.

A model was built to study flashing flow in a nozzle with the geometry shown in Figure 1, which corresponds to the experimental tests carried out by Abuaf *et al.* (1981), who measured many runs with this geometry. A computational three-dimensional grid was built for the studied geometry, using a structured mesh of 100,000 cells. Mesh sensitivity was tested using a smaller cell size, but no influence on the final results was found. Solid boundaries were represented using no slip velocity conditions. A symmetry boundary was defined in the mirror plane of the nozzle. Inlet and outlet boundary conditions were set to the values of inlet and outlet static pressures of the runs corresponding to Abuaf *et al.* (1981). The turbulence model used was the SST k-ω model, since it provided the best convergence.

The mass flow rate was used to validate the model. The main study was done with the data of run 309 from Abuaf *et al.* (1981), although other runs were also validated, as shown in Table 3, with a difference of the predicted mass flow rate of less than 4%. In run 309, the upstream pressure was fixed at 5.55×10^6 Pa and the downstream pressure at 3.78×10^6 Pa. The temperature was 420 K and the mass flow 8.80 kg s^{-1}.

The evolution of the pressure (Fig. 7) and the vapor fraction (Fig. 8) in the axis of the nozzle at different temperatures were compared to the pressure and the vapor fraction, respectively, in the experimental essay of Abuaf *et al.* (1981) at a temperature of 420 K. However, this model presents problems of convergence when the temperature approaches the flashing situation. Nevertheless, the prediction of axial pressure and vapor fraction achieved with the best convergence criteria model is in good agreement with the experimental data obtained by Abuaf *et al.* (1981).

The vapor fraction in the symmetry plane of the nozzle at three different temperatures is shown in Figure 9. In the first and the second cases, with temperatures of 373

Table 3. Different runs from Abuaf *et al.* (1981), with the experimental and numerical mass flow values

Run	P_0 (kPa)	T (K)	P_b (kPa)	Mass flow (kg s^{-1})	
				Abuaf	Fluent
122	171.0	373.3	109.2	6.10	6.25
128	248.0	373.1	101.0	9.10	8.78
133	349.0	394.4	205.5	8.93	8.80
148	304.1	393.6	206.0	7.46	7.50
309	555.0	420.0	378.0	8.80	8.75

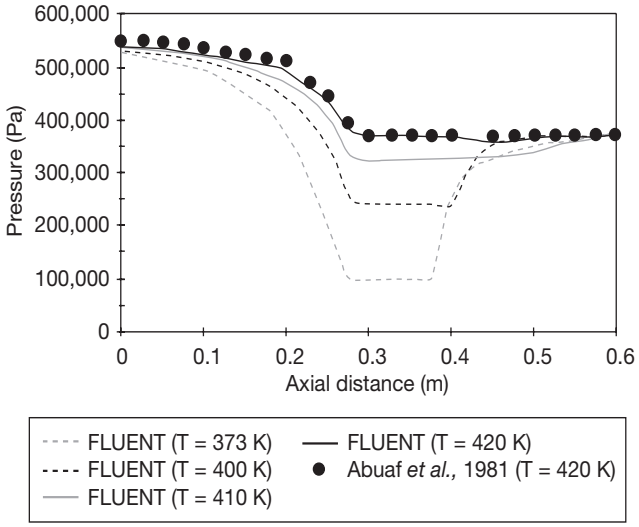

Figure 7. Evolution of the pressure in the axis of the nozzle at different temperatures compared to that of the experimental assay by Abuaf *et al.* (1981).

and 400 K, flashing flow did not develop, although, as expected, cavitation increased with temperature. However, in the third case with a temperature of 420 K, similar to the experimental measured value, flashing flow occurred and the liquid state did not recover. Similar agreement with other runs was obtained at their experimental temperature (Table 3). From all these results, it can be concluded that the new cavitation model of FLUENT V6.1 accurately simulated the flashing flow phenomenon in a nozzle.

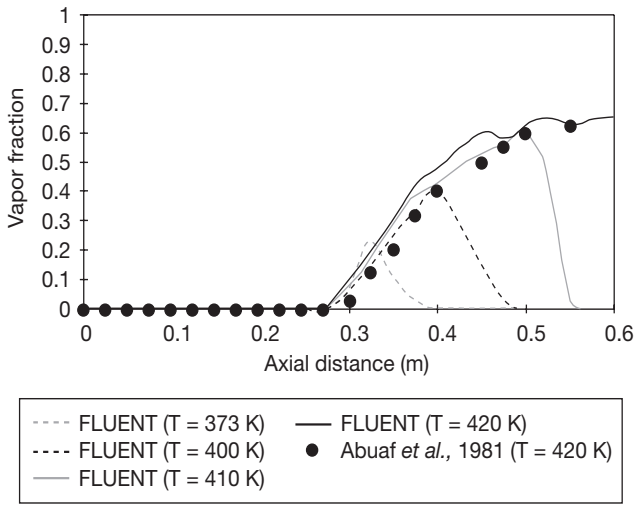

Figure 8. Evolution of the vapor fraction in the axis of the nozzle at different temperatures compared to that of the experimental assay of Abuaf *et al.* (1981) at 420 K.

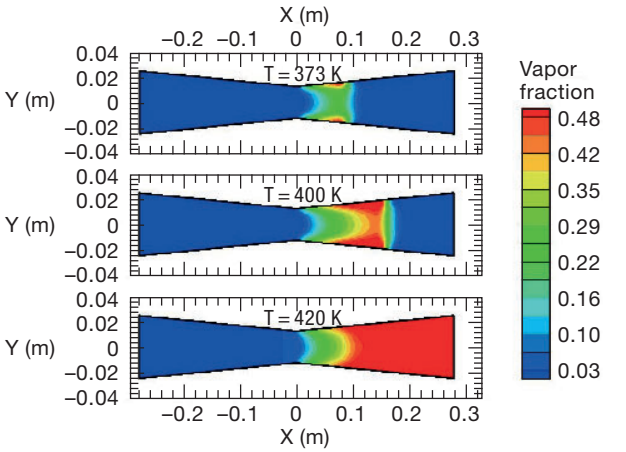

Figure 9. Vapor fraction at different temperatures in the symmetry plane of the nozzle.

Rectangular venturi

This case considered unsteady flow in a rectangular venturi. Experimental data were taken from Stutz and Reboud (2000). A previous numerical study with another commercial code was carried out by Coutier-Delgosha *et al.* (2003). In this study the RNG k-ε and the standard k-ω models were used, which led both to steady situations. However, a modification in the estimation of viscosity for both models improved the simulation of the unsteady cavitation flow.

The geometry of the Venturi used is shown in Figure 1 and was similar to that used in the experimental tests carried out by Stutz and Reboud (2000). This flow is similar to that found in sprinklers (Pascal *et al.*, 2006) or in fertirrigation devices (Manzano and Palau-Salvador, 2005). The turbulence model used was the RNG k-ε model, due to its better convergence compared to other turbulence models assayed. The downstream pressure was fixed at 64,000 Pa and the upstream pressure varied between 2×10^5 and 1×10^5 Pa. The grid was a structured mesh. Several mesh sizes were used for checking grid sensitivity and finally a mesh of 112,000 nodes was selected. Time step was equal to 0.001 s, in accordance with the values obtained in the experimental data.

Figure 10 shows the time variation of the cavitation length after the throat of the Venturi. The cavitation length led to a constant value instead of varying, as had been observed in the experimental tests (Stutz and Reboud, 2000). There were two cycles in which the cavitation length varied, but after the third cycle it reached a steady situation. These results obtained with the new

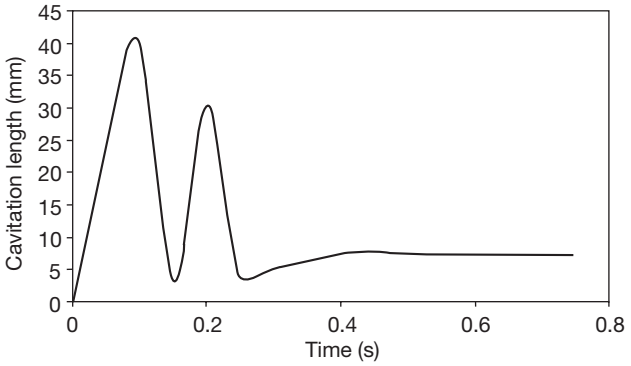

Figure 10. Time variation of the cavitation length after the throat of the rectangular venturi.

cavitation model of FLUENT V6.1 did not improve the results presented by Coutier-Delgosha *et al.* (2003) using the RNG k-ε and the standard k-ω models. This showed that this model did not properly simulate cavitation flow when an unsteady situation was assumed.

Conclusions

Validation studies of the new cavitation model of FLUENT V6.1 have been presented in this paper. The geometries for this validation included a circular orifice, a rectangular orifice and a nozzle, with the assumption of steady flow. A prediction of flashing flow was made in the nozzle geometry. In all cases, good agreement between predictions and experimental data was obtained.

A venturi in an unsteady situation was also studied. In this case, the results obtained from the numerical model did not agree with experimental data and led to a steady situation.

In general, it can be said that the new cavitation model in FLUENT V6.1 provides very reliable simulation of easy geometries when steady flow is assumed.

Acknowledgements

The authors would like to thank Professor Frankel and his research group from Purdue University for their support during the summer of 2003 and 2004. We acknowledge the reviewers for their comments and suggestions. We also thank the R&D&I Linguistic Assistance Office at the *Universidad Politécnica de Valencia* for their help in revising and correcting this paper.

References

ABUAF N., WU B.J.C., ZIMMER G.A., SAHA P., 1981. A study of nonequilibrium flashing of water in a converging-diverging nozzle, NUREG/CR 1864. Office of Nuclear Regulatory Research, BNL-NUREG-51317 – Vol. 1. NY (USA).

CERUTTI S., OMAR M.K., KATZ J., 2000. Numerical study of cavitation inception in the near field of an axisymmetric jet at high Reynolds number. Phys Fluids 12(10), 2444-2460.

COCHARD H., BARIGAH T., HERBERT E., CAUPIN F., 2007. Cavitation in plants at low temperature: is sap transport limited by the tensile strength of water as expected from Briggs' Z-tube experiment? New Phytologist 173, 571–575.

COUTIER-DELGOSHA O., FORTES-PATELLA R., REBOUD J.L., 2003. Evaluation of the turbulence model influence on the numerical simulations of unsteady cavitation. J Fluids Eng 125(1), 38-45.

ELIAS E., CHAMBRE P.L., 2000. Bubble transport in flashing flow. Int J Multiphase Flow 26(1), 191-206.

FARREL K.J., 2003. Eulerian/Lagrangian analysis for the prediction of cavitation inception. J Fluids Eng 125(1), 46-52.

FLUENT, 2001. Fluent user's guide. In: FLUENT V6.1 Manual, Vol. 1-4. Fluent Inc., Lebanon.

KNAPP R.T., DAILY J.W., HAMMIT F.G., 1970. Cavitation. Ed. McGraw-Hill Book Co., Inc., NY, USA. 551 pp.

KUBOTA A., KATO H., YAMAGUCHI H., 1992. A new modelling of cavitation flows: a numerical study of unsteady cavitation on a hydrofoil section. J Fluids Mech 240(1), 59-96.

LAUNDER B.E, SPALDING D.B., 1972. Lectures in mathematical models of turbulence. Academic Press, London. 169 pp.

MAHERALI H., MOURA C., CALDEIRA M., WILLSON C., JACKSON R., 2006. Functional coordination between leaf gas exchange and vulnerability to xylem cavitation in temperate forest trees. Plant Cell Environ 29, 571-583.

MANZANO J., PALAU-SALVADOR G., 2005. Hydraulic modelling of venturi injector by means of CFD. ASABE Annual International Meeting, Tampa, Florida.

MEYER R.S., BILLET M.L., HOLL J.M., 1992. Freestream nuclei and travelling bubble cavitation. J Fluids Eng 114, 672-679.

MUÑOZ-COBO J.L., CEREZO E., VERDU G., 2000. Development and validation of EVAPCOND1D-1 and EVAPCOND1D-2 models for the flashing phenomena in pipes of variable area. AMIF-ESF Computing methods for two-phase flow. Aussois, France.

NORTON T., SUN D., 2006. Computational fluid dynamics (CFD) – an effective and efficient design and analysis tool for the food industry: a review. Trends Food Sci Tech 17, 600-620.

NORTON T., SUN D., GRANT J., FALLON R., DODD V., 2007. Applications of computational fluid dynamics (CFD) in the modelling and design of ventilation systems in the agricultural industry: a review. Bioresource Technol 98, 2386-2414.

NURICK W.H., 1976. Orifice cavitation and its effect on spray mixing. J Fluids Eng 98, 681-687.

PALAU C.V., ARREGUI F.J., PALAU-SALVADOR G., ESPERT V., 2004. Velocity profile effect on Woltman water meters performance. ICFM International Conference on Flow Measurement. Giulin, China.

PALAU-SALVADOR G., ARVIZA J., BRALTS V., 2004. Flow behaviour through an in-line emitter labyrinth using CFD techniques. ASAE/CSAE Annual International Meeting, Ottawa, Canada.

PALAU-SALVADOR G., BALBASTRE I., GONZÁLEZ-ALTOZANO P., ARVIZA J., 2005. Improvement of the internal geometry of a control valve using CFD. Pipelines 2005. Texas, Houston.

PASCAL M., KADEM N., TCHIFTCHIBACHIAN A., 2006. Investigations on the influence of sprinkler fins and dissolved air on jet flow. J Irrig Drain E-ASCE 132, 41-46.

PATANKAR S.V., 1980. Numerical heat transport and fluid flow. Taylor & Francis, New York. 197 pp.

SINGHAL A.K., ATHAVALE M.M., HUIYING L., JIANG, L., 2002. Mathematical bases and validation of the full cavitation model. J Fluids Eng 124, 617-624.

SMALE N.J., MOUREH J., CORTELLA G., 2006. A review of numerical models of airflow in refrigerated food applications. Int J Refrig 29, 911-930.

STUTZ B., REBOUD J.L., 1997. Experiment on unsteady cavitation. Exp Fluids 22, 191-198.

STUTZ B., REBOUD J.L., 2000. Measurements within unsteady cavitation. Exp Fluids 29, 545-552.

VEERSTEG H.K., MALALASEKERA W., 1995. An introduction to computational fluid dynamics. The finite volume method. Ed. Longman, England. 257 pp.

WEI Q., SHI Y., DONG W., LU G., HUANG S., 2006. Study on hydraulic performance of drip emitters by computational fluid dynamics. Agr Water Manage 84, 130-136.

XING T., 2002. Effect of cavitation on vortex dynamics in a submerged laminar jet. PhD Thesis, Purdue University, West Lafayette, Indiana. 179 pp.

XING T., FRANKEL S.H., 2002. Effect of cavitation on vortex dynamics in a submerged laminar jet. AIAA J, 40, 2266-2276.

XU J.L., CHEN T.K., CHEN X.J., 1997. Critical flow in convergent-divergent nozzles with cavity nucleation model. Exp Therm Fluid Sci 14, 166-173.